

Microstereolithography of lead zirconate titanate thick film on silicon substrate

X.N. Jiang^a, C. Sun^a, X. Zhang^{a,*}, B. Xu^b, Y.H. Ye^b

^a Department of Industrial and Manufacturing Engineering, The Pennsylvania State University, University Park, PA 16802, USA

^b Materials Research Laboratory, The Pennsylvania State University, University Park, PA 16802, USA

Received 16 June 1999; received in revised form 9 May 2000; accepted 10 May 2000

Abstract

The microstereolithography (μ SL) of lead zirconate titanate (PZT) thick films on platinum-buffered silicon substrates is reported for the first time in this paper. Crack-free PZT thick films (80–130 μ m thick) have been fabricated by laser direct-write UV polymerization from the HDDA-based UV curable PZT suspensions. The characterization of the fired films shows dielectric permittivities of 120–200, tangent loss of 0.92–2.5% and remnant polarization of 0.9–1.7 μ C/cm². The field-induced longitudinal piezoelectric coefficient (d_{33}) of an 84- μ m thick film is 100 pC/N and the piezoelectric voltage coefficient (g_{33}) is about 59.5×10^{-3} V m/N. These results demonstrated the potential for μ SL of advanced piezoelectric microsensors and microactuators. © 2000 Elsevier Science B.V. All rights reserved.

Keywords: Microstereolithography; PZT; Thick film; Microsensors; Microactuators

1. Introduction

Lead zirconate titanate (PZT) films on silicon substrate have been considered very promising for microsensors and actuators with high energy density [1–3]. PZT thick films (> 15 μ m) are of special interest in developing microsensors and actuators with high power output, such as micropumps, micromotors and ultrasonic microtransducers [4–7]. Various PZT film deposition techniques have been developed in the past decade (Table 1) [8–15]. However, the reported PZT thick film deposition approaches, such as screen printing and jet printing, utilize mechanically contacted pattern mode, leading to a limited thick film pattern resolution of about 50 μ m. In addition, multiple paste-heating-cooling cycles are usually required in the above-mentioned thick film processes, since the single paste pass can only yield about 10 μ m thick film within each cycle

(printing, binder burning, firing, cooling) [5]. Therefore, the slow deposition rate is also a concern in these processes.

A rapid 3D microfabrication technology, microstereolithography (μ SL), was recently introduced to fabricate high aspect ratio and complex 3D-microstructures for MEMS [16]. The μ SL shares the same principle with its macroscale counterpart, but in different dimensions. In μ SL, a UV laser beam can be focused to 1–2 μ m, rather than hundreds of microns in conventional SL to obtain precisely patterned microstructures. With synchronized x - y beam scanning and z -axis motion, the complicated 3D micropart can then be built in a layer-by-layer fashion (Fig. 1).

The fabrications of micropolymeric parts and subsequent electroplating of micrometallic parts have been explored [16–19]. Impressively, most of the complex 3D microparts with high aspect ratio can be built within a few hours [16]. Recently, successful μ SL of structural ceramics was reported in the fabrications of 400 μ m and 1 mm alumina gears [17]. In order to further improve the μ SL fabrication speed, some modified μ SL approaches by using optical fibers [18] and dynamic mask generators have

* Corresponding author. Current address: Department of Mechanical and Aerospace Engineering, 37-144 Engineering IV, University of California, Los Angeles, CA 90095, USA.

E-mail address: xiang@seas.ucla.edu (X. Zhang).

Table 1
PZT film fabrication approaches

Processes	Deposition rate (thickness)	Composition control	Compatibility with IC process
EB evaporation	Intermediate	Bad	Good
IB deposition	Low	Intermediate	Good
Sol-gel	Low	Good	Intermediate
Hydrothermal reaction	Intermediate	Intermediate	Bad
Sputtering	~ 1 $\mu\text{m}/\text{h}$, low	Intermediate	Good
Laser ablation	1–3 $\mu\text{m}/\text{h}$, intermediate	Good	Good
Jet printing	High	Bad	Bad
Screen printing	~ 100 μm , high	Intermediate	Intermediate
Electrophoretic deposition	Intermediate	Intermediate	Bad

also been developed [19], allowing for rapid fabrication of microparts on large silicon wafers.

To fabricate the PZT thick film structures on silicon substrate in a rapid and precise way for advanced piezoelectric microdevices, a novel μSL process with high pattern resolution and rapid prototyping nature is developed in this study. Structural and physical properties of the fabricated PZT thick films are characterized and compared with those of the films fabricated by other methods.

2. μSL of PZT thick films

Due to the fact that ceramic suspension is quite viscous at high solid loading (volume fraction), the previous free-surface μSL apparatus cannot be used effectively for the film re-coating and thickness control [17]. A precision blade technique was developed to spread the suspension into a uniform layer with controlled thickness ranging from several microns to hundreds of microns, which is defined by the distance between the blade and substrate. The modified μSL apparatus consists of the following major components: an Ar^+ laser, a beam delivery system, computer-controlled precision x - y - z stages, and a blade with a precision micrometer (Fig. 1). The smallest UV beam spot size achieved was 1–2 μm . The laser wavelength used in this work was 364 nm.

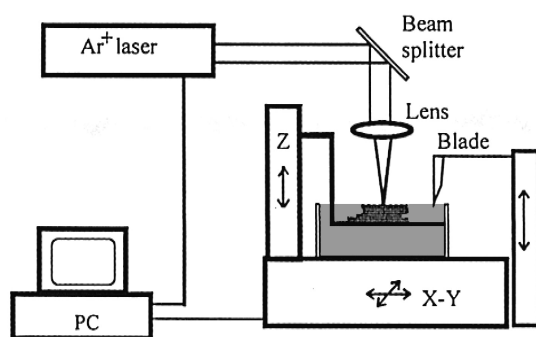


Fig. 1. The developed μSL apparatus including an Ar^+ laser, the beam delivery system, computer-controlled precision x - y - z stages and precision blade.

The UV curable PZT suspension was prepared by ball milling fine PZT powders (EDO 76), UV curable monomer (1,6-hexabediol diacrylate (HDDA)), photoinitiator, solvent and dispersant. The mean particle size of PZT powders was about 1 μm before ball milling. The solution was diluted with solvent to achieve reasonable viscosity. The addition of dispersant and the ball milling were used to homogenize the suspension. Generally, the highly loaded ceramic suspension is quite viscous, unless an excellent degree of colloidal dispersion is achieved [20]. Considering a ceramic suspension viscosity of 3000 $\text{mPa}\cdot\text{s}$, which was set as the maximum resin viscosity in conventional SL to ensure a satisfactory layer re-coating [21]. The relationship between the solid loading (volume fraction) of HDDA-based suspension and the dispersion factor dispersion is shown in Fig. 2, calculated from the Krieger–Dougherty equation [20]. Dispersion factor is a coefficient used to

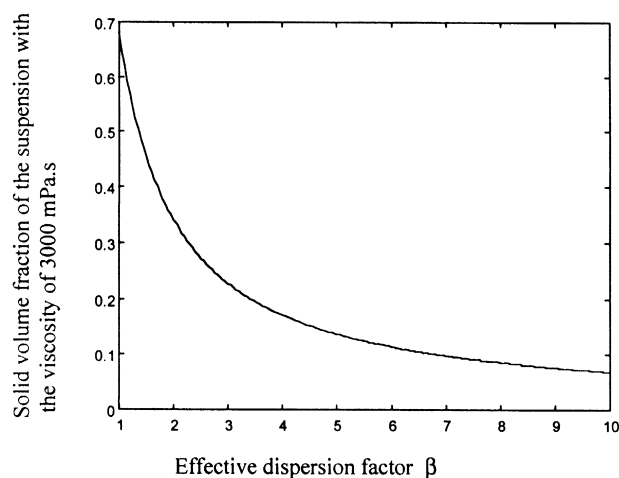


Fig. 2. The relationship between the maximum solid volume fraction and the dispersion factor in the case where the suspension viscosity is equal to 3000 $\text{mPa}\cdot\text{s}$, the viscosity limitation for stereolithography (Krieger–Dougherty equation: $\nu = \nu_0(1 - \beta\Phi/\Phi_0)^{-2.5\Phi_0}$, where ν is the viscosity of suspension; ν_0 is the viscosity of pure liquid ($\nu_0 = 6 \text{ mPa}\cdot\text{s}$ for HDDA); β is the dispersion factor (≥ 1), $\beta = 1$ with perfect dispersion; Φ is the solid volume fraction; Φ_0 is the maximum solid fraction in the case of perfect dispersion ($\Phi_0 = 0.7$ for powders with a wide particle size distribution)).

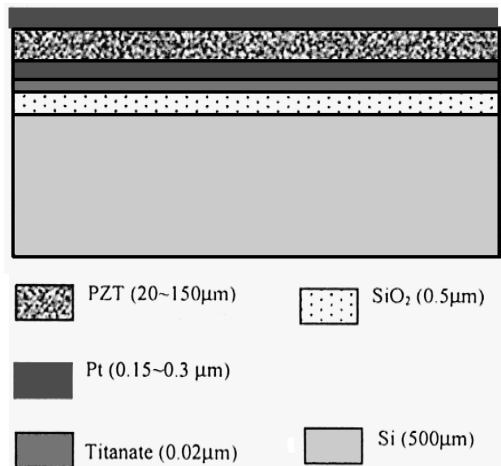


Fig. 3. Schematic cross-view of PZT thick film on Pt-buffered silicon substrate.

measure how well the particles are dispersed in the solutions, and it is equal to 1 when the particles are perfectly colloidally dispersed, otherwise, it is larger than 1. In this work, the solid loading of the prepared HDDA-based PZT suspension was 33% (vol.). The 500- μm -thick silicon wafer was prepared with a 500-nm thermally grown oxide, sputter-coated 150-nm platinum and a 20-nm titanium adhesion layer (Fig. 3). The silicon substrate was placed on the elevator, which was attached to the z stage.

PZT thick films ($> 15 \mu\text{m}$) were then fabricated on Si substrate with the μSL apparatus. A PZT suspension layer with controlled thickness was uniformly spread on the substrate by a precision blade. The film was then solidified and patterned after the subsequent UV laser exposures. The unpolymerized PZT suspension was removed by rinsing the wafer carefully with isopropyl alcohol (IPA) and DI water for several minutes. It was dried with compressed air and put into a post-curing box for 30 min to 1 h. After the post-curing, the films were heated slowly at a ramp of

$2^\circ\text{C}/\text{min}$ to 300°C where it was held for 2 h, then further heated up to 650°C and held for 4 h to burn out all the binders (polymer), followed by annealing at $700\text{--}850^\circ\text{C}$ for 1–2 h. Finally, 200–300 nm Pt film was sputtered on the top of PZT film as the top electrode (Fig. 3).

3. Characterization

The μSL fabricated PZT thick films on silicon substrate were characterized by investigating the microstructure and physical properties, such as dielectric and piezoelectric properties. An Alpha-Step 100 profilometer was used to measure the film thickness, the measurement accuracy of this equipment for the thickness measurement is 0.1 and 2.5 nm corresponding to the measurement range of less than 13 and over 13 μm , respectively. The X-ray diffraction (XRD) patterns of the crystal structure of the fabricated PZT thick films were recorded by a Scintag DMC-105 diffractometer. The microstructure and morphology of the film were observed by a scanning electron microscope (SEM). The capacitance and loss tangent were measured directly by a Hewlett Packard 4274A LCR meter at 1 kHz. The dielectric permittivity was then calculated by $\epsilon = Ct/(\epsilon_0 S)$, where C is the capacitance, t is the thickness of the PZT film, S is the electrode area, and ϵ_0 is the permittivity of a vacuum. The ferroelectric hysteresis behavior of the film was examined with a modified Sawyer–Tower circuit at 50 Hz driving field, from which the coercive field, remnant polarization and maximum polarization can be determined. The piezoelectric properties of the film were evaluated from the strain response to a weak external-driving field. The mechanical properties of the PZT films formed would also be of interest for the future work. A modified double-beam laser interferometer, which is capable of resolving AC displacement of the order of 0.001 nm with a lock-in amplifier [22], was used

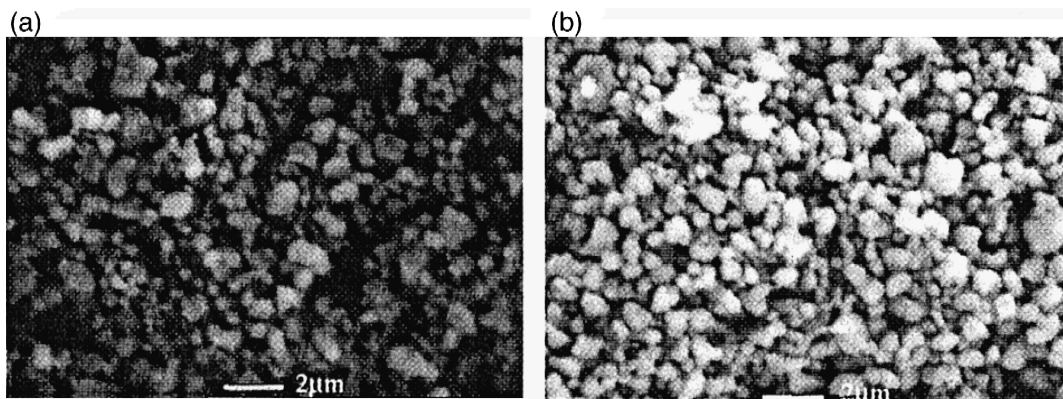


Fig. 4. SEM surface microstructure of the fabricated thick PZT film (100 μm). (a) Microstructure of green PZT thick film (PZT powders and binders (HDDA)); (b) microstructure of PZT thick film after burning and 1 h annealing under the peak temperature of 850°C .

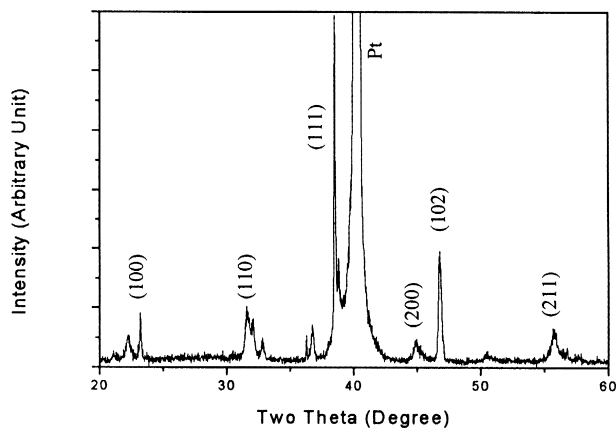


Fig. 5. XRD pattern of PZT thick films fired at 850°C for 1 h. The wafer structure consisted of 0.5- μm -thick thermally grown oxide on silicon, with 20 nm of titanium for adhesion and 0.15 μm platinum as bottom electrode/diffusion barrier.

to measure the longitudinal strain, χ . The longitudinal piezoelectric coefficient, d_{33} , was then calculated through the converse piezoelectric effect, defined as $\chi = d_{33}E$, where E is the applied electric field. The piezoelectric voltage coefficient, defined by $g_{33} = d_{33}/(\epsilon_0 \epsilon)$, was then derived from the measured d_{33} and dielectric permittivity of the films.

4. Results and discussions

The PZT thick films on silicon substrate were successfully fabricated by μSL from HDDA-based PZT suspension. By changing the laser energy density, the solidified PZT lines were 20–100 μm wide and 10–150 μm thick. It is known that the ceramic curing depth, C_d , is inversely proportional to the square of refractive index difference between the ceramic particles and the UV curable solution, Δn , as $C_d \propto 1/(\Delta n)^2$ [23,24]. The large refractive index difference between the UV curable solution and ceramics

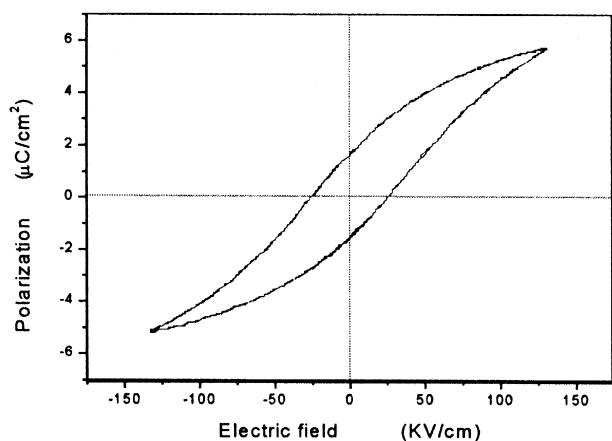


Fig. 6. Polarization-applied field hysteresis for an 84- μm -thick PZT film at 50 Hz.

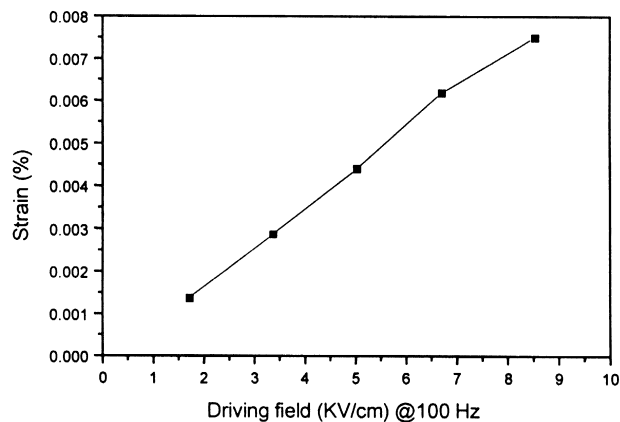


Fig. 7. Field-induced longitudinal strain vs. applied driving field. The thickness of PZT film is 84 μm annealed at 850°C for 1 h and subsequently at 700°C for 2 h, coercive field is 26.1 kV/cm .

results in the decrease in curing depth, and the significant laser light scattering into the lateral direction, which causes larger line width. To improve the precision in μSL of highly concentrated suspension, a modified UV curable ceramic suspension with UV absorber was developed in this work. An experiment was conducted to fabricate discs of 150 μm in diameter from 55 vol.% ceramic suspensions with and without UV absorber, but under the same laser exposure of 111.5 μW and the same layer thickness of 20 μm . It was found that the fabricated disk is about 155 μm in diameter in the case of with UV absorber, in contrast to the 220 μm diameter without UV absorber. This demonstrated that UV absorber could significantly reduce the light scattering and hence increase the resolution.

After the binder burning and annealing process with a slow heating and cooling ramp, crack-free PZT thick films on silicon substrate were achieved, from the observation, with thickness ranging from 50 to 130 μm . For the fabrication of a PZT film with the planar sizes of 2×4 mm, 4 min was required with a laser beam scanning speed

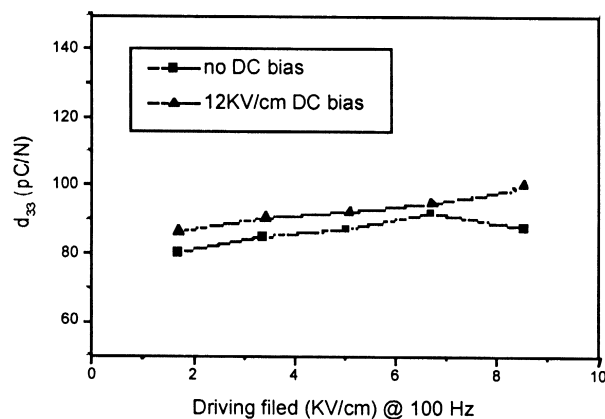


Fig. 8. Piezoelectric strain coefficient d_{33} as a function of applied fields without DC bias and with a DC bias of 12 KV/cm . The thickness of the PZT film is 84 μm , while the coercive field is 26.1 kV/cm .

Table 2
Property comparison of PZT thick film on Si substrate

PZT thick film processes	Film thickness (μm)	Dielectric constant	Tangent δ	d_{33} (pC/N)
Screen printing [7] ^a	12	200	0.05	50
μSL	84	200	0.01	100

^aThe thermal treatment condition is almost the same as the one used in this work.

of 3.32 mm/s and a line space of 10 μm . Faster fabrication can be achieved by using projection μSL [19].

The microstructures of the fabricated green PZT thick film and the film after firing are compared in Fig. 4(a) and (b), respectively. The green film is found to be less dense with polymers occupying the pores between solid particles and acting as binders, which is due to the relatively low solid loading used (33 vol.%). After burning and annealing, the grains grow resulting in a denser PZT film. However, the grains are still relatively small since the annealing temperature (850°C) used is far below the typical sintering temperature (1200°C) where the firing of the PZT films on buffered silicon results in blistering of the titanium/platinum underlayer [5]. The XRD pattern of the PZT thick film annealed at 850°C indicated the formation of a single-phase perovskite structure (Fig. 5).

The dielectric and ferroelectric properties of the fabricated PZT thick films were characterized at room temperature. The dielectric constant of the films is 127–200, with the tangent losses of 0.92–2.5% at 1 kHz. A typical polarization-applied field hysteresis measured in the fabricated PZT thick films is shown in Fig. 6. The remnant polarizations of 0.93–1.67 $\mu\text{C}/\text{cm}^2$ are comparable with that of PZT thick films fabricated by other processes [5,15]. The coercive fields of 26–45 kV/cm were determined under the peak fields of 107–162 kV/cm. It was observed that additional 2-h 700°C annealing yielded a higher dielectric constant. In addition, more efficient barrier layers between silicon substrate and PZT film will allow longer annealing time at higher temperature (950–1000°C) to obtain denser films and improve the film properties [5].

The longitudinal piezoelectric coefficient, d_{33} , of the PZT film was determined by measuring the longitudinal strain under an external field. The AC strain response of an 84- μm -thick PZT film under different driving fields at 100 Hz is shown in Fig. 7, and the slope of the line corresponds to d_{33} , which is about 88.7 pC/N. The effect of applying an electric field with DC bias on the d_{33} of the films was also investigated. The effective d_{33} measured under driving fields with 12 kV/cm DC bias was found to be higher than that without DC bias (Fig. 8). This can be explained by the fact that the polarization of the film increases with bias until saturation, and the polarization contributes directly to the longitudinal coefficient [5]. The

maximum d_{33} of 100 pC/N of the μSL fabricated PZT thick films was about twice that of the PZT thick films fabricated by other methods (Table 2) [5,14], although it is still below the bulk PZT material value of 583 pC/N. The relatively low dielectric constant and remnant polarization of the PZT thick films formed resulted from the fact that low annealing temperature and relatively low solid loading (33% vol.) of PZT suspension prepared for μSL lead to the less dense film [5]. However, with the measured d_{33} and the dielectric constant, the piezoelectric voltage coefficient, g_{33} , is derived as 59.5×10^{-3} V m/N, which is three times larger than the bulk PZT value of 19.1×10^{-3} V m/N. The measured d_{33} and g_{33} demonstrated that the PZT thick films on silicon substrate by μSL hold good potential for both microactuators and microsensors applications.

5. Conclusions

For the first time, crack-free PZT thick films (50–130 μm thick) have been successfully deposited on silicon substrate by using μSL . The microstructural, dielectric and piezoelectric properties of the fabricated PZT films have been investigated. The measured d_{33} (100 pC/N) and g_{33} (59.5×10^{-3} V m/N) of the fabricated PZT thick films are promising for advanced piezoelectric microsensors and actuators. The microfabrication process, μSL of PZT thick films on silicon substrate, can be integrated with the conventional silicon micromachining processes. Current efforts are focusing on property enhancement by increasing the solid loading in PZT suspension and optimizing the post-processes for μSL fabricated PZT thick films.

Acknowledgements

The authors wish to thank Prof. Joseph Dougherty, Dr. K. Yao and Ms. Chiping Wang of Materials Research Laboratory in Penn State University for their helpful discussions. The authors also acknowledge EDO Ceramics in the US for the PZT powders supply.

References

- [1] S. Thakoor, J.M. Morookian, The role of piezoelectric microactuation for advanced mobility, Proc. IEEE Micro Electro Mech. Syst. '96 (1996) 205–211.
- [2] D.L. Polla, L.F. Francis, Ferroelectric thin films in microelectromechanical systems applications, MRS Bull. 21 (7) (1996) 59–65, July.
- [3] J.F. Lindberg, The application of high energy density transducer materials to smart systems, Mater. Res. Soc. Symp. Proc. 459 (1997) 509–519.
- [4] A.M. Flynn, L.S. Tavrow, S.F. Bart, R.A. Brooks, D.J. Ehrlich, K.R. Udayakumar, L.E. Cross, Piezoelectric micromotors for micro-robots, J. Microelectromech. Syst. 1 (1) (1992) 44–51.

- [5] H.D. Chen, K.R. Udayakumar, L.E. Cross, J.J. Bernstein, L.C. Niles, Dielectric, ferroelectric, and piezoelectric properties of lead zirconate titanate thick films on silicon substrates, *J. Appl. Phys.* 77 (7) (1995) 3349–3353.
- [6] M. Koch, A.G.R. Evans, A. Brunnscheiler, The dynamic micropump driven with a screen printed PZT actuator, *J. Micromech. Microeng.* 8 (1998) 119–122.
- [7] J.J. Bernstein, S.L. Finberg, K. Houston, L.C. Niles, H.D. Chen, L.E. Cross, Micromachined high frequency ferroelectric sonar transducers, *IEEE Trans. Ultrason. Ferroelectr. Freq. Control* 44 (5) (1997) 960–969.
- [8] M. Oikawa, K. Toda, Preparation of Pb(Zr, Ti)O₃ thin films by an electron beam evaporation technique, *Appl. Phys. Lett.* 29 (8) (1976) 491–492.
- [9] R.N. Castellano, L.G. Feinstein, Ion-beam deposition of thin films of ferroelectric lead zirconate titanate (PZT), *J. Appl. Phys.* 50 (6) (1979) 4406–4411.
- [10] T. Tuchiya, T. Itoh, G. Sasaki, T. Suga, Preparation and properties of piezoelectric lead zirconate titanate thin films for microsensors and microactuators by Sol–Gel processing, *J. Ceram. Soc. Jpn.* 104 (3) (1996) 159–163.
- [11] K. Shimomura, T. Tsurumi, Y. Ohba, M. Daimon, Preparation of lead zirconate titanate thin film by hydrothermal method, *Jpn. J. Appl. Phys.* 30 (9B) (1991) 2174–2177.
- [12] M. Mescher, T. Abe, B. Brunett, H. Metla, T.E. Schlesinger, M. Reed, Piezoelectric lead zirconate titanate actuator films for micro-electromechanical systems applications, *Proc. IEEE Micro Electro Mech. Syst.* '95 (1995) 261–266.
- [13] R. Maeda, K. Kikuchi, A. Schroth, A. Umezawa, S. Matsumoto, Deposition of PZT thin films by pulsed laser ablation for MEMS application, *SPIE* 3242 (1997) 372–379.
- [14] A. Schroth, M. Ichiki, R. Maeda, J. Akedo, Characterization and application of Jet-printed thin PZT layers for actuation of MEMS, *SPIE* 3242 (1997) 380–387.
- [15] J. Van Tassel, C.A. Randall, Thin/thick piezoelectric films by electrophoretic deposition, *SPIE* 3324 (1998) 14–19.
- [16] K. Ikuta, K. Hirowatari, Real three dimensional microfabrication using stereo lithography and metal molding, *Proc. IEEE Micro Electro Mech. Syst.* '93 (1993) 42–47.
- [17] X. Zhang, X.N. Jiang, C. Sun, Micro-stereolithography of polymeric and ceramic microstructures, *Sens. Actuators, A*, in press.
- [18] K. Ikuta, T. Ogata, S. Kojima, Development of mass productive micro stereo lithography, *Proc. IEEE Micro Electro Mech. Syst.* '96 (1996) 301–305.
- [19] A. Bertsch, H. Lorenz, P. Renaud, Combining microstereolithography and thick resist UV lithography for 3D microfabrication, *Proc. IEEE Micro Electro Mech. Syst.* '98 (1998) 18–23.
- [20] I.M. Krieger, T.J. Dougherty, A mechanism for non-Newtonian flow in suspensions of rigid spheres, *Trans. Soc. Rheol.* 3 (1959) 137–152.
- [21] M.L. Griffith, J.W. Halloran, Freeform fabrication of ceramics via stereolithography, *J. Am. Ceram. Soc.* 79 (10) (1996) 2601–2608.
- [22] W.Y. Pan, L.E. Cross, A sensitive double beam laser interferometer for studying high-frequency piezoelectric and electrostrictive strains, *Rev. Sci. Instrum.* 60 (1989) 2701–2705.
- [23] M.L. Griffith, J.W. Halloran, Scattering of ultraviolet radiation in turbid suspension, *J. Appl. Phys.* 81 (6) (1997) 2538–2546.
- [24] C.L. Haertling, S. Yoshikawa, R.E. Newnham, Thick film patterned ceramics using UV-curable pastes, *J. Am. Ceram. Soc.* 73 (11) (1990) 3339–3344.

Biographies

Xiaoning Jiang received his PhD from Tsinghua University, Beijing, China in 1996. He joined Nanyang Technological University in Singapore in 1996 as a post-doctoral fellow. He is now a post-doctoral scholar at the Micro-manufacturing Laboratory (μ ML) in the Pennsylvania State University. His current research interests include high-aspect-ratio microfabrication, microfluidic systems, and smart materials for microactuators and MEMS.

Cheng Sun received his Masters degree in Condensed Matter Physics in 1996. He is now a PhD student in the Industrial and Manufacturing Engineering Department. His major research interest is microfabrication.

Xiang Zhang graduated with a PhD in Mechanical Engineering from University of California, Berkeley in 1996 and MS/BS in Physics from Nanjing University. He joined Pennsylvania State University in 1996 as an assistant professor and directs Penn State's Micro-manufacturing Laboratory (μ ML). His past research experiences include: microthermal wave sensor design and fabrication, ferroelectric liquid crystal phase transition, high- T_c superconductivity, laser processing of semiconductor materials. His current research interests are: 3D micromachining, microstereolithography for MEMS, and microsensors and actuators.

Baomin Xu received his PhD degree in Ceramics from Shanghai Institute of Ceramics, Chinese Academy of Sciences in 1994. He is currently a Research Associate at the Materials Research Laboratory of the Pennsylvania State University. His research interests include preparation and application of ferroelectric thin and thick films, piezoelectric materials and devices for sensor, actuator and transducer applications, and dielectric materials. He is a member of the American Ceramic Society and the Materials Research Society.

Yaohong Ye received her ME degree in Electronic Materials from the University of Electronic Science and Technology of China. She is currently working at the Materials Research Laboratory of the Pennsylvania State University as a visiting scholar. Her research interests include the preparation of ferroelectric thin and thick films, and their applications in microelectromechanical systems.